

OVERVIEW OF BEAM DIAGNOSTIC SYSTEMS FOR FRIB*

S.M. Lidia[#], S. Cogan, D. Constan-Wahl, J. Crisp, M. Ikegami, Z. Liu, F. Marti, I. Nesterenko, E. Pozdeyev, T. Russo, R. Shane, R.C. Webber, Y. Zhang, Q. Zhao, Facility for Rare Isotope Beams East Lansing, Michigan, USA

Abstract

The Facility for Rare Isotope Beams will extend the intensity frontier of heavy ion linac facilities, with continuous beam power up to 400 kW and beam energy ≥ 200 MeV/u. Strict demands are placed on the beam diagnostics in the front end, linac, and beam delivery systems to ensure delivery of high quality beams to the target with minimal losses. We describe the design of diagnostic systems in each accelerator sector for commissioning and operations.

INTRODUCTION

Facility for Rare Isotope Beams (FRIB) is a high-power, high-brightness, heavy ion facility under construction at Michigan State University under cooperative agreement with the US DOE [1]. The linac will accelerate ions to energies above 200 MeV/u, with up to 400 kW of beam power on target. The linac facility, shown in Fig. 1, consists of a Front End, three Linac Segments (LSs) connected by two Folding Segments (FSs), and a Beam Delivery System (BDS) leading to the production target [2].

CHALLENGES FOR BEAM INSTRUMENTATION

FRIB employs a superconducting linac to accelerate the high power, high brightness hadron beam. As such, it shares operational issues with other facilities (SNS, ESS, RHIC, LHC, JPARC, etc.) with regards to power handling, cleanliness of components, restricted access to the beam line, prohibitions against actuated diagnostics near cryomodules, etc. Additional challenges for beam instrumentation presented by FRIB include the low energy of the heavy ion beams, the folded linac geometry, and the plan to transport and accelerate multiple charge states simultaneously.

Low-beta Beam Position Monitoring

The relatively low velocity of the ion beams in the driver linac has implications for accurate beam position monitoring. With low β , the electric field lines spread out resulting in longer, slower image current, and reduced high frequency content. The significance of this effect depends on the proximity to the button and it results in frequency response dependent on position and velocity [3][4][5].

*This material is based upon work supported by the U.S. Department of Energy Office of Science under Cooperative Agreement DE-SC0000661, the State of Michigan and Michigan State University.
#lidia@frib.msu.edu

Multiple Charge State Beams

The acceleration, transport and delivery of a multiple charge state composite beam presents particular complications to the beam instrumentation design and functionality necessary to establish the machine tune. Representative ion species for FRIB are listed in Table 1, where Q1 is the beam charge state in the Front End and LS1, and Q2 is the beam charge state following the stripper and charge selector in FS1. In the case of Uranium, two charge states are transmitted to the stripper, with five states selected for additional acceleration and target delivery.

Table 1: Representative Ion Species in FRIB

Ion Species	A	E _{max} (MeV/u)	Q1	Q2-center	Q2-spread
U	238	200	33, 34	78	76-80
Xe	136	221	18	49	48-50
Kr	86	257	14	35	35
Ca	48	264	11	20	20
Ar	36	320	8	18	18
O	16	320	6	8	8

In LS1, orbit oscillations in both longitudinal and transverse phase space arise due to charge state dispersion ($\Delta Q/Q$) in neighboring rf buckets. A challenge to beam instrumentation is to spatially resolve the phase dispersion of the charge states so that the oscillation can be monitored, and growth in both longitudinal and transverse emittance be minimized. This may be accomplished by utilizing the network of linac BPMs and incorporating digital sampling techniques to determine the oscillation phase.

Large Dynamic Range of Beam Intensity

The FRIB linac is designed to support multiple operating modes with varying time structure and peak intensity of the ion beams. These modes can be grouped into four general categories:

- Short pulse ($< 5 - 50 \mu\text{s}$), low duty cycle ($< \sim 1$ Hz), varying intensity (50 to 650 μA)
- Moderate pulse length (~ 0.01 s to s), low duty cycle ($< \sim 1$ Hz), nominal intensity ($\sim 650 \mu\text{A}$)
- Approximately CW (50 μs gap @ 100 Hz), low to nominal intensity (< 10 to 650 μA)

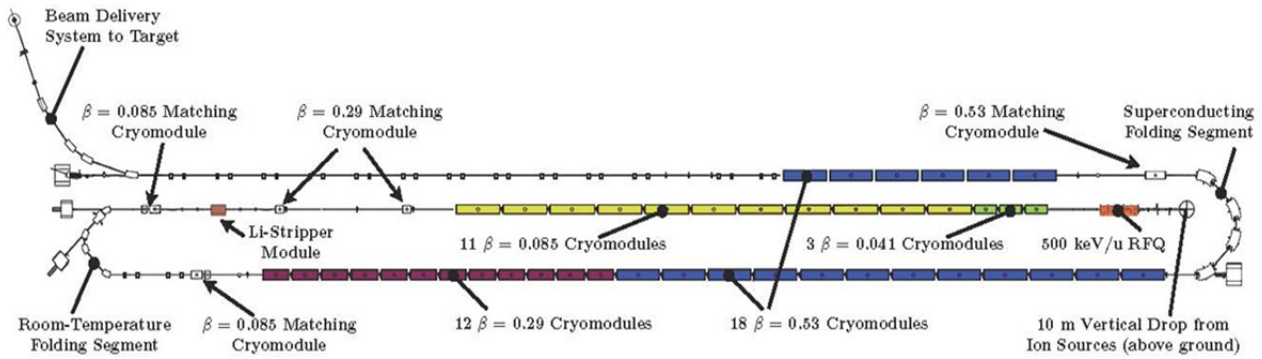


Figure 1: Schematic layout of FRIB drive accelerator facility.

- Dynamic ramp to high power (variable intensity, pulse duration, and repetition rate) to slowly increase the target temperature (~30 s for warm re-start to 10 minutes for cold start).

Several modes used for commissioning the front end and fragment separator lack quantitative definition, but may be mapped to one of the other categories. These modes exhibit a wide range in intensity (2 – 650 μA for Front End commissioning, and 0.0001–30 pA for fragment separator commissioning and secondary beam development).

The previously discussed beam modes define the range of conditions that the beam instrumentation must serve. Beam instrumentation is required to detect beam currents ranging from ~1 mA to ~1 μA , with bandwidths sufficient to provide sensitivity over many orders of magnitude in duty cycle or pulse duration (CW to 50 μs pulse duration at 1 Hz). Additional operating modes, albeit a small fraction of the operating schedule, require lower peak intensities and average beam power. The baseline resolution requirements for the diagnostic systems assume CW operation with 100 μA beam current. Operationally, for reduced average beam currents, longer integration or averaging times may be used to restore resolution. In the extreme case of ion beam fluxes ~100 pA, intercepting diagnostics may be utilized with long integration times to acquire flux density information on the transported beams.

Machine Protection System

The high power and brightness, and short (< mm) Bragg range of the FRIB heavy ion beam places critical importance on the fast protection system to detect and protect against prompt beam losses [6]. The performance and lifetime of sensitive superconducting cavity surfaces can be affected by small losses (< 1 W/m) occurring over long durations.

The twice-folded geometry of the FRIB linac places the high energy linac segment in close proximity to the low energy linac segment. Traditional loss monitors, eg. ionization chambers and scintillation-based neutron detectors, will be unable to differentiate the relatively low-amplitude loss signals arising in LS1 from the high-

amplitude signals generated in LS3 due to radiation cross-talk [7]. Additionally, x-ray background sources originating from the RF cavities themselves can also potentially overwhelm the beam-generated signals in the low energy linac modules.

OVERVIEW OF BEAM DIAGNOSTIC INSTRUMENTATION

The suite of beam instrumentation systems is designed to facilitate initial commissioning and tuning activities preceding user operations, and to monitor beam transport and acceleration function and provide sensors for machine protection during operations. Diagnostic systems will be provided to continuously measure beam position and orbit deviations, beam current and transmission at several points, and beam loss induced radiation fields. On-demand diagnostics will produce measurements of beam phase space densities, bunch duration, 1-D beam profiles and 2-D transverse (x-y) or hybrid (x-z) distributions. Time of flight measurements using a dense network of beam position monitors will enable phase and amplitude tuning for all RF cavities in the linac sections [8].

Overall Requirements and Sensitivities

To meet the demands of the FRIB experimental systems, stringent requirements on the linac driver and beam delivery system are imposed. These are summarized in Table 2.

Table 2: Required Beam Parameters at Target for Five-Charge-State Uranium

Parameter	Value	Required (% beam)
Beam spot size	1 mm	$\geq 90\%$
Angular spread	± 5 mr	$\geq 90\%$
Bunch duration	3 ns	$\geq 95\%$
Energy spread	$\pm 0.5\%$	$\geq 95\%$

FRONT END

The instrumentation package in the Front End section will enable selection and tuning of two charge states to be simultaneously accelerated and transported to the first linac segment, while maintaining beam quality. The two

ion source lines in the FRIB front-end (Fig. 2) will each include a diagnostic station, capable of intercepting up to 300 W of continuous beam power, comprising (i) horizontal and vertical charge-selecting slits; (ii) a Faraday cup; (iii) view screen and optics; and (iv) horizontal and vertical Allison scanners [9].

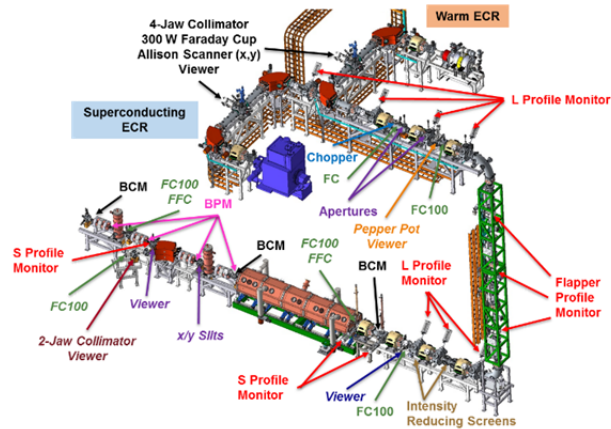


Figure 2: Schematic of diagnostic systems in the FRIB Front End.

The Low Energy Beam Transport (LEBT) beamline transports and manipulates the beam between the ion source and charge selector, and the RF quadrupole accelerator (RFQ). The initial stage of the LEBT uses an electrostatic, deflecting chopper to limit the beam pulse duration and to impress an ~ 100 Hz intensity modulation on the otherwise CW beam. Following the chopper are collimating apertures to remove off-angle beam tails and limit the beam emittance along the modulated pulse. A sequence of 1-D profile monitors (Fig. 3) and pepperpot emittance monitor support analysis of the beam quality and assurance that the transport lattice and beam distribution are well matched. Following the multi-harmonic buncher and velocity equalizer [8], a pair of fast Faraday cups (BW 5-10 GHz) will be utilized to monitor the longitudinal distribution prior to injection to the RFQ, and to the downstream linac section..

AC-coupled beam current transformers (ACCTs) [10] continuously monitor the beam transmission through the RFQ and at the exit of the MEBT. A 50 μ s, 100 Hz current notch or beam gap is imposed by the chopper so that the current baseline can be periodically recovered with the ACCTs. Beam position monitors (BPMs), tuned to a harmonic of the 80.5 MHz cavity frequency, are introduced following the RFQ. Nearly all BPMs in the FRIB lattice use 20-mm diameter buttons to sense the beam [3].

LINAC SEGMENTS

The first linac segment (LS1) accelerates the two-charge-state ion beam from 500 keV/u to 16 MeV/u. Beam position monitors are located both within the cryomodule assemblies, between superconducting solenoids and RF cavities (Fig. 4), and in the warm

sections between cryomodules (Fig. 5). In the two higher energy linac segments (LS2 and LS3), BPMs are located only in the warm sections between cryomodules.

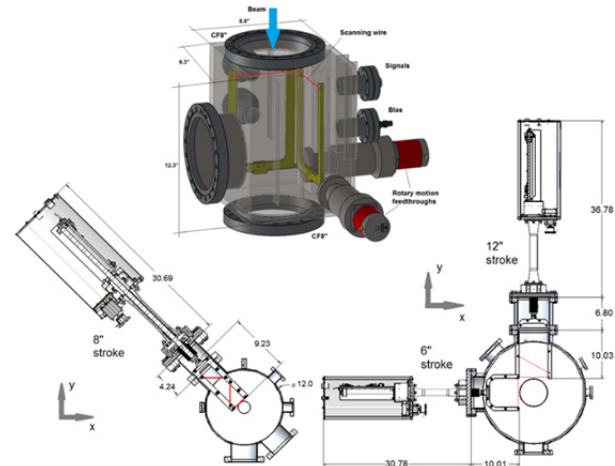


Figure 3: FRIB wire profile monitors. Flapper (top), Small (left), Large (right).

There are a total of 39 cold BPMs integrated with the LS1 cryomass assemblies. Steel jacketed, ceramic dielectric (SiO_2), 50 Ohm cables are used within the cryomodule insulating vacuum to carry the BPM signals from the ~ 4 K beam line to a 300 K feedthrough. The small cable diameter (0.090 inch) limits the static heat load presented to the cryogenic system. This system has been installed on the prototype FRIB 0.085 cryomodule cold mass, and verified with a network analyser at ambient and cryogenic temperatures [11].

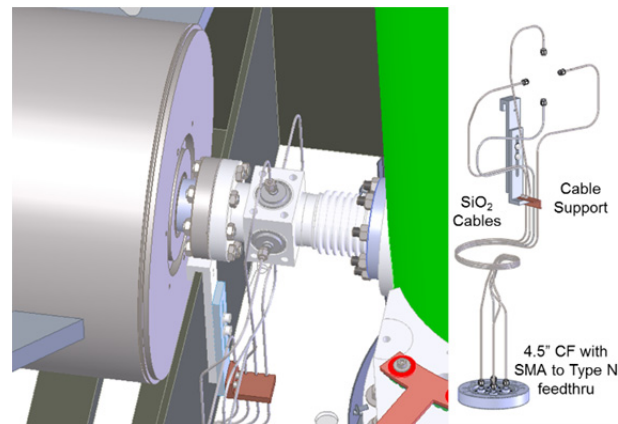


Figure 4: Cryogenic BPM installed between solenoid and cavity in LS1 (left), and cryogenic cable assembly (right).

All FRIB BPMs will be mapped with a purpose-built stretched wire, RF-driven test stand. Polynomial correction removes geometric nonlinearities from the difference-over-sum algorithm, providing position error $< 100 \mu\text{m}$ over $\sim 2/3$ of the BPM aperture.

RF phase referencing for each BPM will be accomplished with a dedicated tap from the local (10.625

MHz) RF reference line. Each BPM reference is transmitted along with the individual BPM button signals in a bundle of 5 phase matched cables to a common digitizer board. A custom analog board (based on the FRIB LLRF board) will be used to condition and digitize the input signals, which will then be passed to the FRIB General Purpose Digital Board (FGPDB) for signal processing and reporting. This system will be incorporated within a MTCA.4 standard chassis.

Beam current monitors are installed along each straight section in the folded linac. These are Bergoz AC current transformers (ACCTs) with ~300 kHz high frequency cutoff. An integral Hereward feedback circuit extends the low frequency response to ~3 Hz yielding a 100 ms *L/R* time constant. The positions of the current monitors have been optimized to reduce residual DC magnetic fields from nearby, large bore magnets. Additional magnetic shielding is added to further reduce the effects of stray flux that limit the low frequency response.

Halo Monitor Rings [7] with apertures closely matching the physical apertures of the cryomodules are installed in the warm sections between cryomodules (Fig. 5). They are capacitively-coupled to the electrical ground of the diagnostic box and provide a measurement of intercepted current (down to ~10 nA) whether from halo scraping or transverse excursions of the beam core. Current work is examining the optimum ring aperture as a compromise between detection sensitivity, tuning flexibility, and ring lifetime.

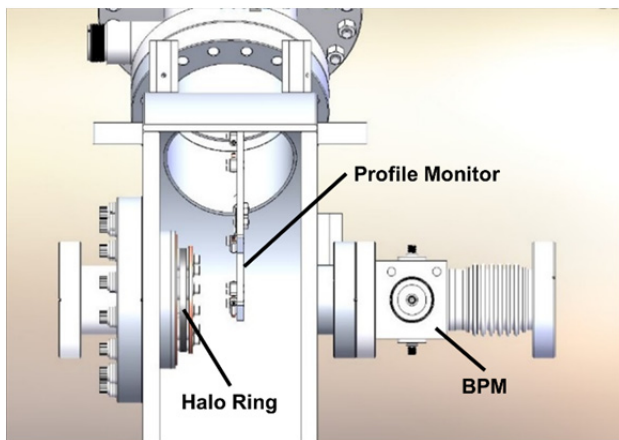


Figure 5: Warm section diagnostic box, with wire profile monitor, BPM, and halo monitor ring. The profile monitor (shown) is absent in stations between cryomodules.

External beam loss monitors (ionization chambers and scintillator-PMT-based, moderated neutron detectors) will be placed along LS3 and the high energy end of LS2 for prompt detection of x-rays and gammas, and for more sensitive detection of neutron fluxes.

A fast thermometry system [12] will be installed within the cryomodules in LS1 and the low energy portion of LS2 to provide enhanced beam loss detection. Pairs of resistance temperature detectors (RTDs) will be installed at the entrance and exit of each cryogenic solenoid in

these cryomodules to detect changes in local temperature from deposited beam power. Fast (~10 kHz) signal conditioning and digitizing modules provide sensitivity to 0.1 K temperature changes on a seconds-order time scale.

FOLDING SEGMENTS AND BEAM DELIVERY SYSTEM

The low energy (~16 to 20 MeV/u) Folding Segment 1 (FS1, see Fig. 6) serves several purposes: (i) to provide a warm magnet transport lattice to connect LS1 to LS2; (ii) to strip the ions in the beam to a higher charge state; (iii) to select up to five charge states for transport and injection in LS2; and (iv) to provide a straight-ahead beam dump line for commissioning and tuning LS1. A second beam dump in FS1 facilitates tuning the charge state selector and beam optics. The high energy (≥ 150 MeV/u) Folding Segment 2 (Fig. 7) provides a transport lattice with four superconducting dipole magnets to connect LS2 to LS3, as well as a straight ahead beam dump for LS2 commissioning and tuning.

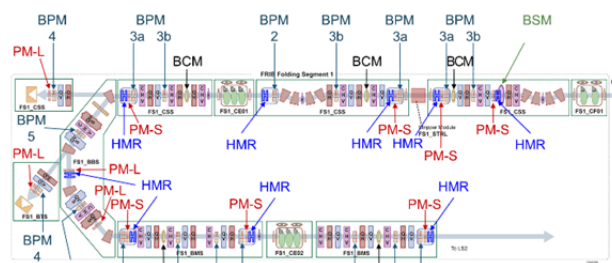


Figure 6: Ideogram of Folding Segment 1.

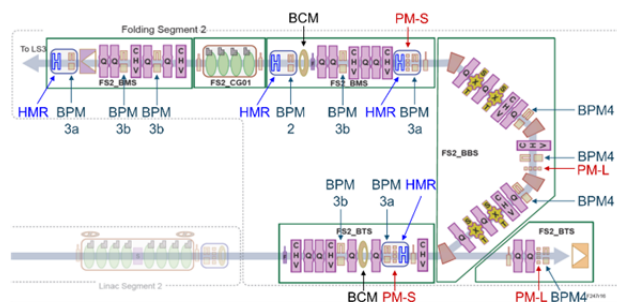


Figure 7: Ideogram of Folding Segment 2.

A separate issue with multi-charge state beams arises in the Folding Segments due to dispersion. In FS1, the beam distribution at the BPM following the charge selector is dispersed horizontally by up to ~80 mm. A large (150 mm) aperture, elliptical, split plate BPM design (Fig. 8) provides a larger linear response aperture [13].

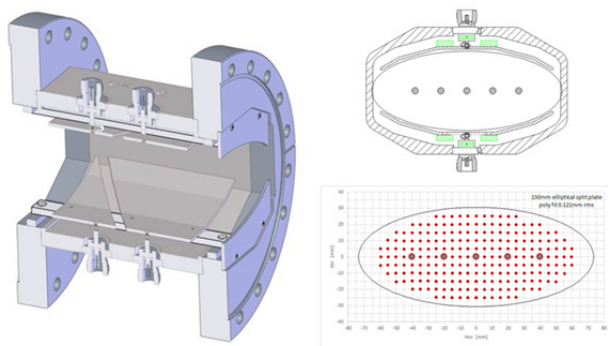


Figure 8: 150 mm, large aspect ratio BPM in dispersive section of FS1 (left). (Right) BPM cross-section and linearized response map with multi-charge-state beam component positions indicated.

Additional BPM instrumentation is required to provide beam tuning capability in the Folding Segments. Custom vacuum chambers within specific quadrupole magnets will incorporate BPMs (Fig. 9).

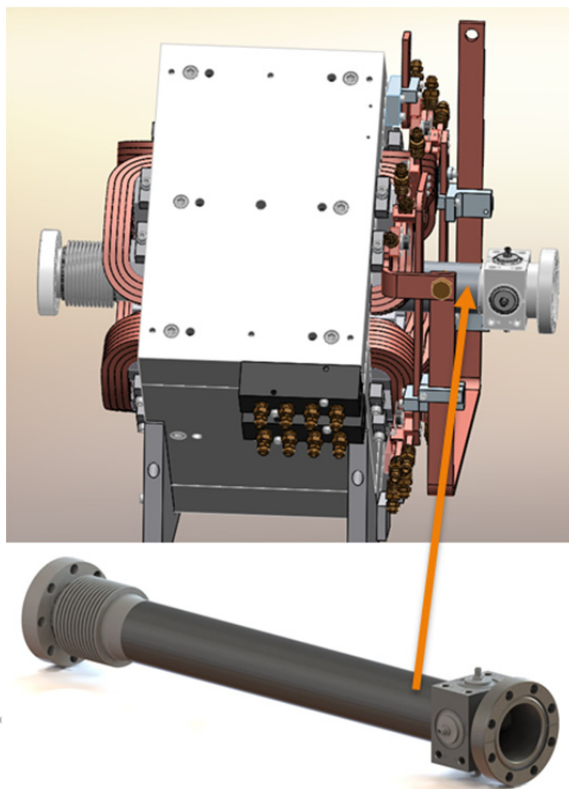


Figure 9: (Top) Vacuum chamber with integrated BPM in quadrupole magnet (FS1, FS2). (Bottom) Type 3b BPM assembly.

The basic instrumentation suite includes beam position monitors, transverse profile monitors, and beam current monitors. The charge stripper imposes requirements on the incoming beam distribution to minimize the resulting energy spread and beam emittance growth. A Feschenko-type bunch shape monitor [14] will be used to monitor the

transverse and longitudinal bunch profile and to enable upstream tuning to match the beam on to the stripper foil or curtain.

The final transport lattice, the Beam Delivery System (BDS), delivers the multi-charge-state beam to the target with parameters as given in Table 1. The BDS beam instrumentation design includes beam position, transverse profile, and beam current monitoring. A full energy, ≥ 200 MeV/u, straight ahead beam dump is used for commissioning and tuning of LS3 and the linac-to-BDS transport line. This dump however is not rated for full beam power.

REFERENCES

- [1] J. Wei, et al., "FRIB accelerator status and challenges", LINAC'12, Tel Aviv, August 2012, p. 417; <http://www.JACoW.org>
- [2] F. Pellemoine, et al., "Development of a production target for FRIB: therm-mechanical studies", J. Radioanal Nucl Chem, DOI 10.1007/s10967-013-2623-7.
- [3] O. Yair, et al., "FRIB beam position monitor pick-up design", Proceedings of IBIC2014, Monterey, USA, TUPF16; <http://www.JACoW.org>
- [4] A. Lunin, et al., "Development of a low-beta button BPM for the PXIE project", Proceedings of IBIC2013, Oxford, UK, TUPC14; <http://www.JACoW.org>
- [5] R.E. Shafer, "Beam position monitor sensitivity for low- β beams", AIP Conf. Proc. 319 (1994).
- [6] S. Lidia, "Diagnostics for high power accelerator machine protection systems", Proceedings of IBIC 2014, Monterey, CA; <http://www.JACoW.org>
- [7] Z. Liu, et al., "A new beam loss detector for low-energy proton and heavy-ion accelerators", Nucl. Instrum. Methods Physics Res. A767 (2014), 262.
- [8] Q. Zhao, et al., "FRIB accelerator beam dynamics design and challenges", Proceedings of HB2012, Beijing, China, WEO3B01; <http://www.JACoW.org>
- [9] P.W. Allison, et al., IEEE Trans. Nucl. Sci. NS-30, (1983), 2204.
- [10] <http://bergoz.com/>
- [11] S. Miller, et al., "Construction and Performance of FRIB Quarter Wave Prototype Cryomodule", SRF'15, Whistler, Canada (2015).
- [12] D. Orris, et al., "Fast thermometry for superconducting rf cavity testing," Proceedings of PAC07, WEPMN105; <http://www.JACoW.org>
- [13] E. Schulte, in *Beam Instrumentation*, J. Bossler (ed.), CERN-PE-ED 001-92.
- [14] Feschenko A.V., Ostroumov P.N. "Bunch Shape Measuring Technique and Its Application For an Ion Linac Tuning", *Proc. of the 1986 Linear Accelerator Conference*, Stanford, 2-6 June, 1986, pp. 323-327.